pubs.acs.org/acschemicalbiology

Articles

A Cell-Free Gene Expression Platform for Discovering and Characterizing Stop Codon Suppressing tRNAs

Kosuke Seki, Joey L. Galindo, Ashty S. Karim, and Michael C. Jewett*

Cite This: *ACS Chem. Biol.* 2023, 18, 1324−1334

Read Online

ACCESS | Metrics & More | Article Recommendations | Supporting Information

ABSTRACT: Non-canonical amino acids (ncAAs) can be incorporated into peptides and proteins to create new properties and functions. Site-specific ncAA incorporation is typically enabled by orthogonal translation systems comprising a stop codon suppressing tRNA (typically UAG), an aminoacyl-tRNA synthetase, and an ncAA of interest. Unfortunately, methods to discover and characterize suppressor tRNAs are limited because of laborious and time-consuming workflows in living cells. In this work, we develop an*Escherichia coli* crude extract-based cell-free gene expression system to rapidly express and characterize functional suppressor tRNAs. Our approach co-expresses orthogonal tRNAs using endogenous machinery alongside a stop-codon containing superfolder green fluorescent protein (sfGFP) reporter, which can be used as a simple read-out for suppression. As a model, we evaluate the UAG and UAA suppressing activity of several orthogonal tRNAs. Then, we demonstrate that co-transcription of two mutually orthogonal tRNAs can direct the incorporation of two unique ncAAs within a single modified sfGFP. Finally, we show that the cell-free workflow can be used to discover putative UAG-suppressor tRNAs found in metagenomic data, which are nonspecifically recognized by endogenous aminoacyl-tRNA synthetases. We anticipate that our cell-free system will accelerate the development of orthogonal translation systems for synthetic biology.

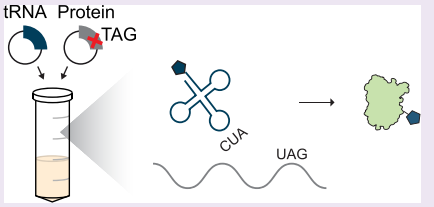

INTRODUCTION

Peptides and proteins are extraordinary classes of sequence-defined polymers made from amino acids. The sequence and chemistry of the amino acids provide a broad range of functions. While there have been many advances in using the canonical twenty amino acids to engineer or evolve new functions within proteins and peptides,[1] non-canonical amino acids (ncAAs; defined as those outside the canonical twenty) often remain cumbersome to use for those purposes.[2−6] Yet, they have broad potential, as exemplified in studies showing that ncAAs can modulate properties such as enzyme catalysis,[7,8] antibody binding,[9,10] biomaterial properties,[11−14] and therapeutic peptide activity.[15]

A key challenge in site-specific ncAA incorporation is the discovery and characterization of suitable orthogonal transfer RNAs (tRNA) and aminoacyl-tRNA synthetases (aaRS).[16,17] These orthogonal aaRS-tRNA pairs must satisfy stringent requirements, including that they must be independent from endogenous tRNAs and aaRSs but operate in parallel with auxiliary translation factors, elongation factors, and ribosomes. Moreover, they must have sufficient aminoacylation activity to support protein synthesis. Recent studies have discovered several orthogonal aaRS-tRNA pairs that satisfy these criteria, including the engineered *Methanocaldococcus jannaschii* TyrRS-$tRNA^{Tyr}_{CUA}$ pair and several pyrrolysyl (Pyl) PylRS-$tRNA^{Pyl}_{CUA}$ pairs, which are mutually orthogonal.[18−22] This has paved the way for exciting opportunities in the synthesis of proteins containing multiple, distinct ncAAs.[23−26] Additionally, advances in directed evolution strategies have enabled the discovery of more efficient aaRS-tRNA pairs.[27,28] However, laborious and time-consuming workflows in living cells generally impede new discovery and characterization of components required for orthogonal translation systems (OTSs).

Cell-free protein synthesis (CFPS) systems have emerged as powerful approaches for engineering biology.[29] They have been used to rapidly iterate designs for glycosylation pathways,[30] metabolic pathways,[31−33] and therapeutic proteins,[34,35] and they have potential to facilitate discovery and characterization of new OTS components. Indeed, CFPS has already been used to efficiently synthesize proteins containing multiple instances of a single ncAA,[36,37] incorporate a wide variety of ncAAs, including those that are toxic, impermeable across the cell membrane, insoluble, or contain non L-α amino acid backbones,[6,38−43] incorporate multiple, distinct ncAAs into a single protein,[44] reassign sense codons,[45−48] and screen a library of engineered aaRS variants.[49] These advances were enabled by factors such as rapid (<8 h) and high-yielding (>g/L) protein synthesis[37] and the ability to bypass cellular viability constraints.

Received: January 23, 2023
Accepted: May 2, 2023
Published: May 31, 2023

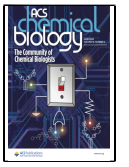

https://doi.org/10.1021/acschembio.3c00051
ACS Chem. Biol. 2023, 18, 1324−1334

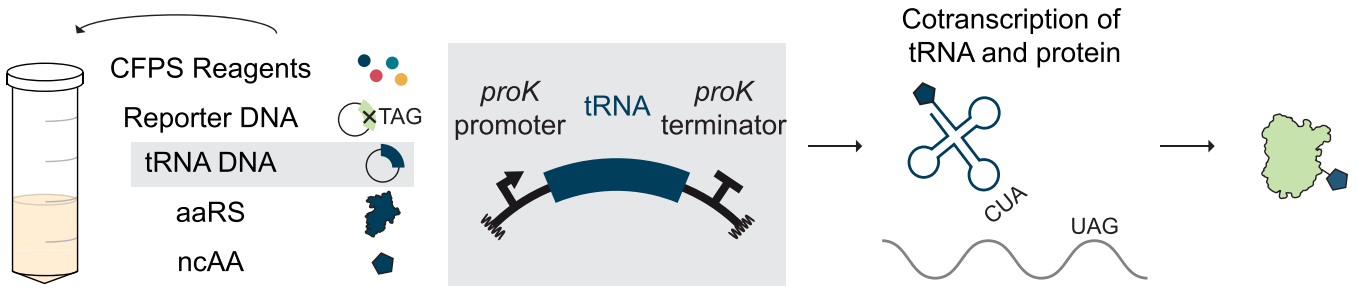

Figure 1. Cell-free gene expression platform for discovering and characterizing tRNAs in CFPS. Orthogonal tRNAs are expressed from an endogenous *proK* promoter, which drives expression of a 216UAG-superfolder green fluorescent protein (sfGFP) reporter.

However, one challenge in cell-free systems for OTS development is the expression of suppressor tRNAs. To express ncAA-containing proteins, CFPS typically requires cell extracts that are pre-enriched with orthogonal tRNAs by overexpression *in vivo* or addition of tRNAs purified by traditional *in vitro* transcription methods. Both methods are unfavorable for tRNA discovery and characterization efforts, as they require time-consuming cell growth or tRNA purification steps. One approach that is amenable to discovery is to co-express suppressor tRNAs alongside a reporter protein. Indeed, in extracts that were pre-enriched with *M. jannaschii* $tRNA^{Tyr}_{CUA}$, additional tRNA supplied by co-transcription of a "transzyme" construct using T7 RNA polymerase improved yields in a CFPS reaction.[50] While powerful for expressing individual proteins, this method generally faces several drawbacks, including the necessity to design unique hammerhead ribozyme sequences for each tRNA,[51] the potential for inefficient cleavage or expression of tRNAs leading to low protein yields, and decreased flexibility due to the use of enriched extracts.

To address these limitations, we present a modular and efficient cell-free method to enable rapid expression and evaluation of stop codon suppressing tRNAs. We first designed and optimized endogenously driven constructs enabling tRNAs to be co-transcribed with mRNA templates for ncAA-containing proteins of interest in naïve extracts (Figure 1). The tRNA construct contains a *proKE. coli* promoter and terminator on a plasmid template, allowing for tRNA expression and maturation. Next, we show that this method is generalizable for expression and evaluation of a panel of commonly used UAG- and UAA-suppressing tRNAs that were chosen for their mutual orthogonality.[18,19,52] We use these mutually orthogonal tRNAs to incorporate multiple, distinct ncAAs into a single protein by *in situ* transcription of two separate tRNAs. Finally, we use this workflow to screen and characterize a panel of putative UAG-suppressing tRNAs, showing that they are functional UAG suppressors that are substrates for *E. coli* glutaminyl-tRNA synthetase (GlnRS). Our cell-free workflow can be used for future discovery and characterization of tRNAs that may be candidates for incorporating ncAAs into proteins.

RESULTS

We set out to develop a general method for tRNA expression in crude extract-based CFPS reactions. For benchmarking, we first evaluated whether transzymes could be used to transcribe orthogonal tRNAs during CFPS (Figure S1a). This "transzyme" template consists of a buffer sequence, a T7 promoter, a hammerhead ribozyme for transcription of unfavorable 5′ sequences, and a tRNA sequence whose 3′ end terminates the DNA template.[50,51] Linear DNA templates for the *M. jannaschii* $tRNA^{Tyr}_{CUA}$, the *Methanosarcina barkeri* $tRNA^{Pyl}_{CUA}$, the *Methanomethylophilus Alvus* $tRNA^{Pyl}_{CUA}$, and an engineered $^{A}17\ ^{V}C10$ *Int* $tRNA^{Pyl}_{CUA}$, chosen for their mutual orthogonality,[18,19,52] were PCR amplified, purified, and added into CFPS reactions at 30 ng/μL, a concentration previously shown to be optimal.[50] These CFPS reactions consist of 759.T7 extract made from an *E. coli* strain lacking amber codons and Release Factor 1 (RF1),[37] GamS to enable expression of linear DNA templates (Figure S1b),[53] an appropriate ncAA, purified aaRS,[55,56] and tRNA (listed in Table 1), traditional CFPS reagents,[54] and a 216UAG-sfGFP reporter (13.33 ng/μL) containing a premature amber codon at T216 that is terminated by a UAA codon. We found that all transzymes supported 216UAG-sfGFP expression (Figure S1c). Interestingly, 216UAG-sfGFP expression using the *M. jannaschii* $tRNA^{Tyr}_{CUA}$ template did not require GamS for expression, and yields using the *M. alvus* $tRNA^{Pyl}_{CUA}$ were decreased.

Table 1. Description of OTSs and ncAAs Used in This Study

tRNA	ncAA	aaRS
M. jannaschii $tRNA^{Tyr}_{CUA}$	Bipyridyl alanine (Bpy)	BpyRS [55]
M. barkeri $tRNA^{Pyl}_{CUA}$	Azidolysine (AzK)	IPYE Chimeric PylRS [56]
M. alvus $tRNA^{Pyl}_{CUA}$ [18]	AzK	*M. alvus* PylRS [18]
$^{A}17\ ^{V}C10$ *Int* $tRNA^{Pyl}_{CUA}$ [19]	AzK	*Lum1* [19]

We hypothesized that endogenous *E. coli* machinery for tRNA transcription and maturation could be a more general and robust approach because it bypasses the need for hammerhead ribozymes (Figure 1). The *proK* promoter and terminator sequences are often used for orthogonal tRNA expression *in vivo*,[57,58] but it was unclear if these sequences would be functional for tRNA transcription and processing in cell extracts. However, we note that we have previously observed ribosomal RNA processing in extracts.[59]

To test co-transcriptional expression and processing of tRNAs, we first cloned the *M. jannaschii* $tRNA^{Tyr}_{CUA}$ flanked by the *proK* promoter and terminator on a plasmid (Figure S2). CFPS reactions containing 13.33 ng/μL of both the $tRNA^{Tyr}_{CUA}$ and 216UAG-sfGFP plasmid were set up and

https://doi.org/10.1021/acschembio.3c00051
ACS Chem. Biol. 2023, 18, 1324−1334

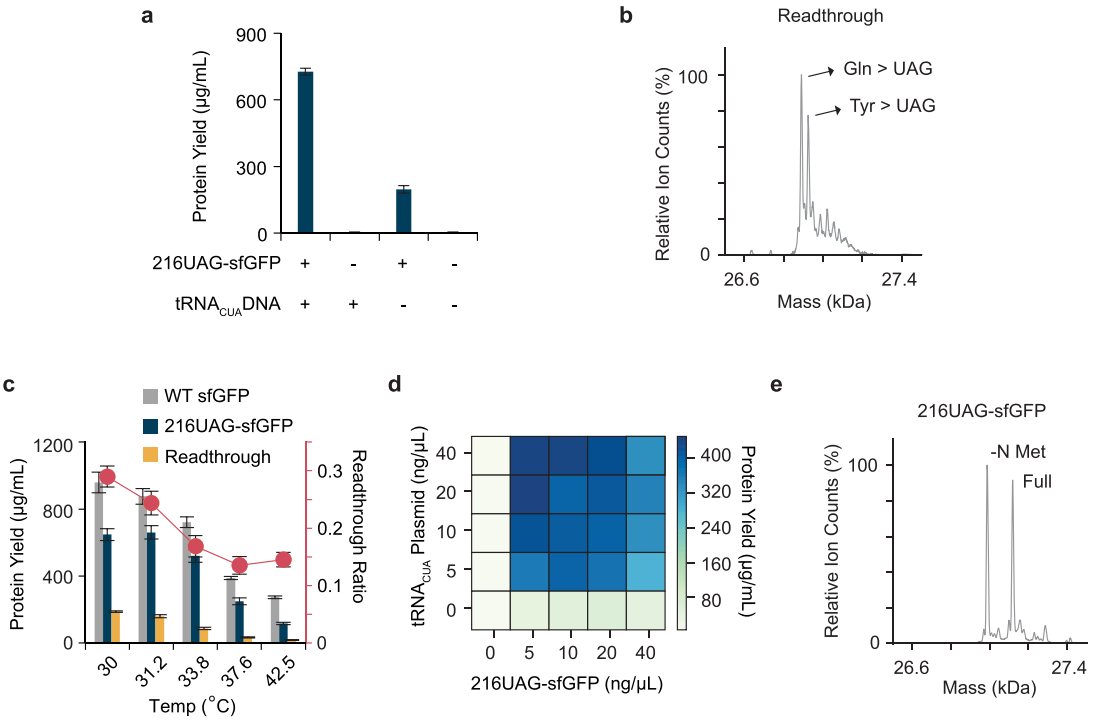

Figure 2. Expression of orthogonal tRNAs from *proK*-based constructs is functional and can be optimized for efficient and accurate ncAA incorporation. (a) Expression of 216UAG-sfGFP is most efficient in the presence of both the 216UAG-sfGFP and tRNA$^{Tyr}_{CUA}$ plasmids. 216UAG-sfGFP expression in the absence of tRNA suggests readthrough by endogenous translation components. Data show the average and standard deviation of three independent replicates. (b) ESI-MS analysis of readthrough products of 216UAG-sfGFP reveals nonspecific incorporation of glutamine and tyrosine. Predicted masses: 26864.23 Da (WT sfGFP), 26892.24 Da (216UAG-sfGFP with glutamine readthrough), and 26926.30 Da (216UAG-sfGFP with tyrosine readthrough). Observed masses: 26890.37, 26924.36 Da. All masses here include the excision of the N-terminal methionine, which is common in *E. coli*. (c) Titration of reaction temperature done in a thermocycler reveals that readthrough is inversely proportional to temperature. Readthrough ratio describes the Readthrough (yellow bars) divided by the 216UAG-sfGFP yields (dark blue bars). Data show the average and standard deviation of three independent replicates. (d) Optimization of plasmid concentrations to reduce unfavorable competition between transcriptional and translational resources improves 216UAG-sfGFP synthesis. Data show the average of three independent replicates. (e) ESI-MS analysis shows accurate ncAA incorporation (Predicted: 26988.22 (-N Methionine) and 27119.42 (Full), Observed: 26988.62 and 27118.65 Da). Mass spectrometry data are representative of at least two independent experiments.

incubated overnight at 30 °C. We measured high yields of ∼725 μg/mL of 216UAG-sfGFP in the presence of both the tRNA$^{Tyr}_{CUA}$ and 216UAG-sfGFP plasmids, showing that tRNAs expressed with endogenous machinery are as efficient as transzyme constructs for amber suppression (Figures 2a and S1c). We also noticed that the addition of the 216UAG-sfGFP plasmid alone resulted in a significant amount of readthrough, which we define as nonspecific suppression of the UAG codon (Figures 2a and S1c). Electrospray-ionization mass spectrometry (ESI-MS) analysis of the intact proteins suggests that readthrough occurs primarily due to nonspecific incorporation of glutamine and tyrosine, which have been previously observed to suppress the UAG codon (Figure 2b).[60] We also found that *proK*-driven expression was nonfunctional when tested with linear templates, likely due to the requirement for supercoiling to activate transcription from these cassettes (Figure S3).[58,61] This precluded a direct comparison with linear transzyme constructs. Nevertheless, these results show amber suppression from transcription and maturation of tRNAs$_{CUA}$ using endogenous machinery in CFPS.

We next aimed to reduce readthrough and optimize expression of 216UAG-sfGFP. Hypothesizing that readthrough in the absence of RF1 results from noncognate base-pairing between the codon and anticodon, we increased the reaction temperature to discourage noncognate base pairing. We found that readthrough and temperature are inversely proportional, and that the readthrough ratio, defined as the quotient between 216UAG-sfGFP yields in the absence and presence of tRNA$^{Tyr}_{CUA}$ DNA, was minimized at higher temperatures (Figure 2c). A reaction temperature of ∼37 °C rather than 30 °C balanced protein yields while maintaining low readthrough and was used for the remainder of UAG suppressing experiments (Figure 2c). To compensate for the loss in yield at 37 °C, we then optimized the ratio of the 216UAG-sfGFP and tRNA$^{Tyr}_{CUA}$ plasmids to reduce unfavorable competition (Figure 2d). A high concentration of *proK*-expressed tRNA template (∼20 ng/μL) and a low concentration of T7-expressed 216UAG-sfGFP template (∼5 ng/μL) produced the highest protein yields. These concentrations were used for the remainder of tRNA expression experiments unless stated otherwise. The synthesized 216UAG-sfGFP product was analyzed by ESI-MS, which displayed a mass shift consistent with ncAA incorporation into 216UAG-sfGFP (Figure 2e). This shows that CFPS reactions can be optimized for relatively high-yielding ncAA incorporation within proteins.

After optimizing our system for tRNA co-expression and ncAA incorporation, we evaluated a panel of other commonly used orthogonal UAG- and UAA-suppressing tRNAs. Suppression of the UGA codon was not studied due to literature suggesting that the UGA codon is subject to readthrough by the *E. coli* tRNA$^{Trp}_{CCA}$.[62,63] To do this, we cloned a panel of orthogonal tRNAs^{Pyl} (Table 1) into the *proK*

https://doi.org/10.1021/acschembio.3c00051
ACS Chem. Biol. 2023, 18, 1324−1334

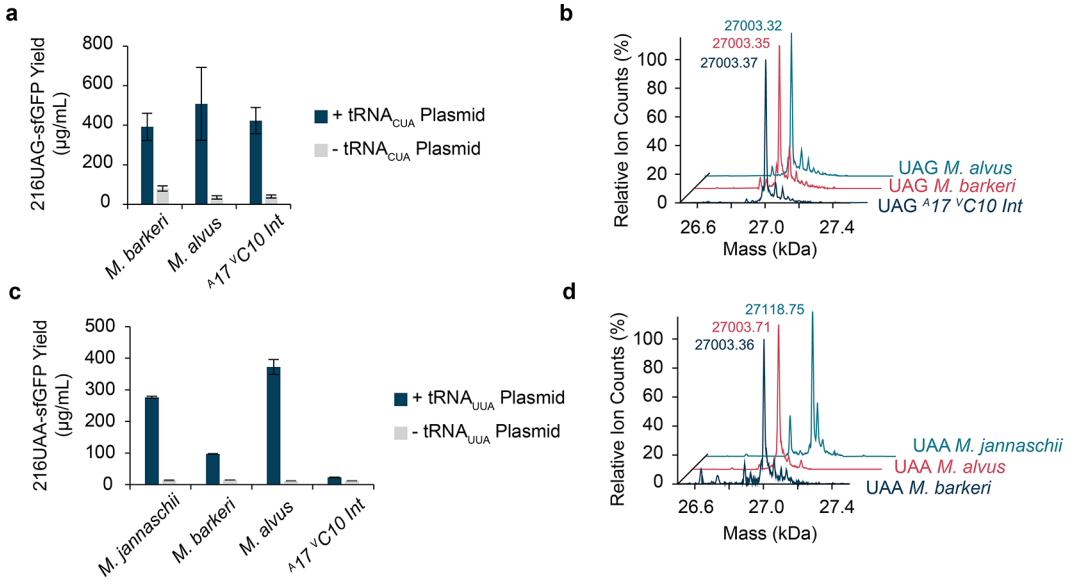

Figure 3. A panel of UAG and UAA suppressing orthogonal tRNAs can be expressed in situ during CFPS. (a) Commonly used tRNAs$^{Pyl}_{CUA}$ support incorporation of AzK. (b) Predicted mass for 216UAG-sfGFP with AzK at T216, 27004.25 Da, is consistent with the observed masses (masses include excision of the N-terminal methionine). (c) Orthogonal tRNAs$_{UUA}$ from M.jannaschii, M. alvus, and *M. barkeri* enables suppression of the 216UAA codon, with a range of observed activities. (d). UAA suppression is confirmed with intact-protein MS. The predicted mass for Bpy incorporation at T216, 27119.42 (including the N-terminal methionine), is consistent with the observed mass, and observed masses for AzK are consistent with the theoretical mass. Data in a and c show the average and standard deviation of three independent replicates (n = 3). Mass spectrometry data are representative of at least two experiments.

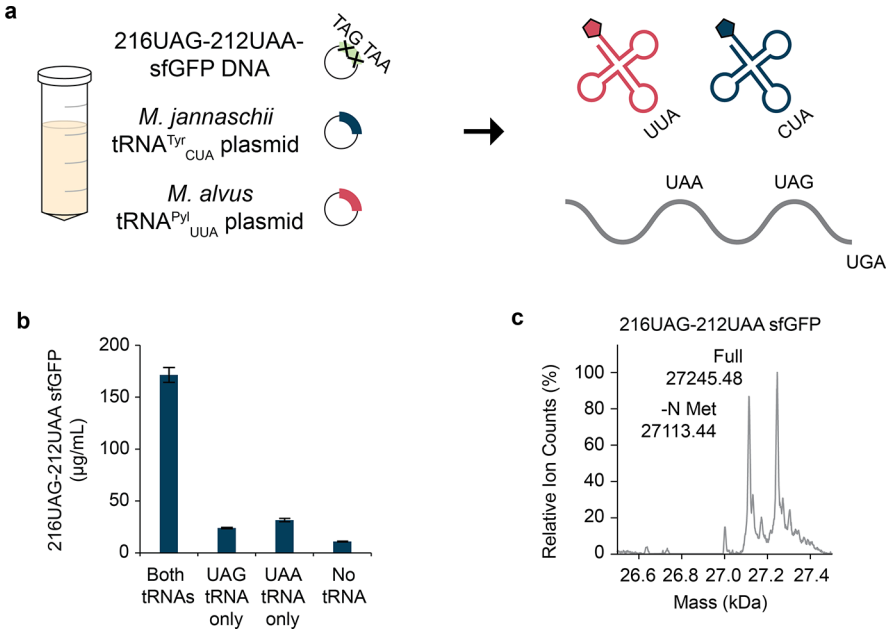

Figure 4. Incorporation of two, distinct ncAAs within a single protein. (a) Schematic for expression of two mutually orthogonal tRNAs. Bpy is being incorporated at the UAG codon and AzK is being incorporated at the UAA codon. (b) Two mutually orthogonal tRNAs can be suppressed within a single protein using a reaction temperature of 30 °C, which was chosen to maximize yields. Both tRNAs are required for efficient full-length protein synthesis. Data show the average and standard deviation of three independent replicates (n = 3). (c) ESI-MS of 216UAG-212UAA sfGFP confirms incorporation of two, unique ncAAs (predicted: 27246.44 (full) and 27115.25 (-NMet)). Mass spectrometry data are representative of two experiments.

cassette and added those plasmids into CFPS reactions. We observed consistent yields of 216UAG-sfGFP across each of the tRNAs$_{CUA}$ in this expression cassette (Figure 3a). ESI-MS analysis shows incorporation of AzK, suggesting efficient tRNA$^{Pyl}_{CUA}$ expression and amber suppression (Figure 3b). We then tested the equivalent tRNAs$_{UUA}$ using a 216UAA-sfGFP reporter, with UAA at the T216 residue and UGA as the terminating codon. The CFPS reactions for UAA suppression were run at 30 °C to enable more efficient protein synthesis as UAA was not expected to suffer from readthrough due to termination by RF2. Interestingly, UAA-suppressing tRNAs exhibited a range of activity (Figure 3c). The 216UAA-sfGFP

https://doi.org/10.1021/acschembio.3c00051
ACS Chem. Biol. 2023, 18, 1324−1334

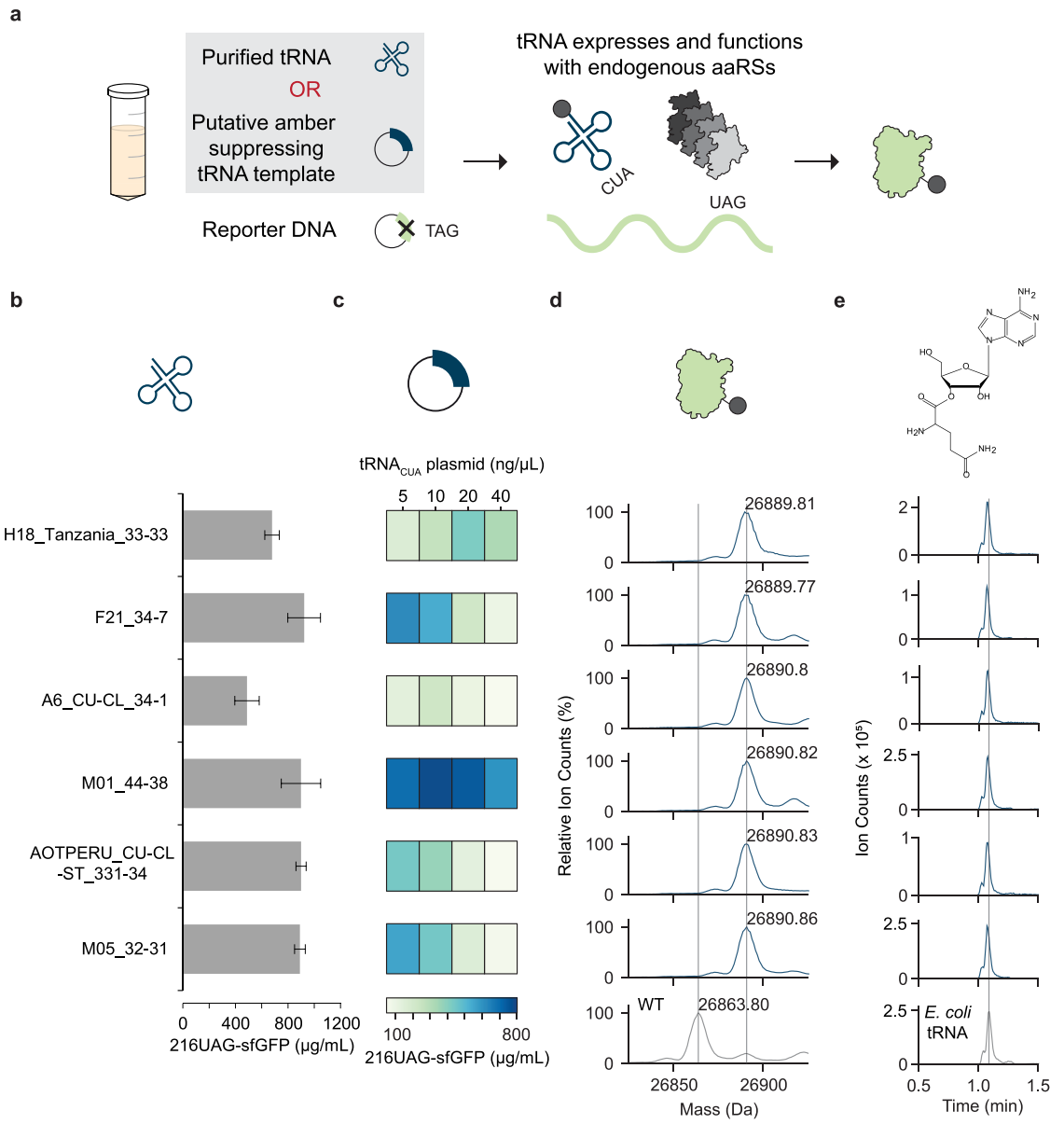

Figure 5. Putative UAG suppressing tRNAs can be expressed and characterized for activity with *E. coli* aaRSs. (a) tRNAs can be expressed and tested for activity with *E. coli* aaRSs. (b) Purified tRNAs are able to support 216UAG-sfGFP synthesis, confirming activity with *E. coli* aaRSs. Data represent the average of three independent replicates, and error bars represent the standard deviation. (c) tRNAs expressed from plasmids containing a *proK* cassette can qualitatively recapitulate activity in (b). Data represent the average of three replicates. (d) ESI-MS analysis of 216UAG-sfGFP from UAG suppressors shows a +27.1 Da mass shift, consistent with T216Q substitution. (Predicted: 26891.25 Da). (e) Extracted ion chromatograms (m = 396.1626 Da) of aminoacylation assays show tRNAs are substrates for *E. coli* GlnRS. All mass spectrometry experiments were repeated with similar results.

yields using the *M. jannaschii* and *M. alvus* tRNAs$_{UUA}$ were relatively high at ∼75 to 80% of 216UAG-sfGFP yields. However, yields of 216UAA-sfGFP were 25% of the 216UAG-sfGFP yields using the *M. barkeri* tRNA$^{Pyl}_{UUA}$ and were negligible for the ^{A}17 ^{V}C10 *Int* tRNA$^{Pyl}_{UUA}$. We also note the low readthrough in these reactions despite being run at 30 °C, likely a result of truncation at UAA by RF2. We confirmed ncAA incorporation at UAA into 216UAA-sfGFP when using the *M. jannaschii*, *M. barkeri*, and *M. alvus* tRNAs$_{UUA}$ by ESI-MS analysis of purified proteins (Figure 3d). These data show that our method for using native tRNA processing in crude cell-free extracts is generalizable toward other tRNAs$_{CUA}$ and can identify functional tRNAs$_{UUA}$.

With several UAG- and UAA-suppressing tRNAs at hand, we next aimed to demonstrate multiple, distinct ncAA incorporation within a single protein using two distinct codons. In this assay, two mutually orthogonal tRNAs would be simultaneously expressed to suppress UAG and UAA (Figure 4a). The *M. jannaschii* tRNA$^{Tyr}_{CUA}$ and the *M. alvus* tRNA$^{Pyl}_{UUA}$ were chosen due to their mutual orthogonality, the anticodon-independent nature of PylRSs,[64,65] and the efficient suppression of UAA by the *M. alvus* tRNA$^{Pyl}_{UUA}$ (Figure 3c). A 216UAG-212UAA-sfGFP reporter, containing UAG at T216, UAA at N212, and UGA as the terminating codon, was successfully synthesized only when both tRNA templates were present (Figure 4b). Small amounts of readthrough were observed in the presence of only a single tRNA, with the

https://doi.org/10.1021/acschembio.3c00051
ACS Chem. Biol. 2023, 18, 1324−1334

$tRNA_{UUA}$ generating slightly higher yields of the readthrough product. This is consistent with the literature suggesting that $tRNAs_{UUA}$ can also readthrough UAG codons.[24,44,66] ESI-MS of the product in the presence of both tRNAs displays mass shifts consistent with the incorporation of each ncAA (Figure 4c). In addition, we confirmed the specificity of each aaRS to its cognate ncAA and tRNA, as listed in Table 1 (Figure S4a,b). This supports the conclusion that the UAG and UAA codons were site-specifically decoded by two unique ncAAs. Thus, co-transcription of two mutually orthogonal tRNAs can direct the incorporation of two unique ncAAs within a single protein.

We next sought to apply our tRNA expression platform toward discovering and characterizing putative UAG-suppressors. Understanding natural UAG-suppressing tRNAs could provide insight into natural mechanisms for genetic code expansion and identify stop codon suppressor tRNAs that may have utility in OTSs. In our method, 216UAG-sfGFP is expressed only when a UAG suppressor is recognized by an endogenous *E. coli* aaRS (Figure 5a). We screened a panel of six putative UAG suppressing tRNAs, which were identified in the genomes of phages that appear to use alternative genetic codes.[67] Sequences for these are provided in Table S4. First, we confirmed that these tRNAs were functional in CFPS by supplementing the reaction with tRNA purified from *in vitro* transcription reactions (Figure 5b). All six tRNAs supported 216UAG-sfGFP synthesis, suggesting that these were functional amber suppressors. Two, A6_CU-CL_34-1 and H18 Tanzania_33-33, were observed to have lower yields. Next, we cloned these sequences into our *proK* expression cassette to test whether cell-free reactions could express these tRNAs. Indeed, using a titration of plasmid concentrations to account for potential differences in expression and to account for potential resource competition (as in Figure 2d), 216UAG-sfGFP expression was observed for all tRNAs (Figure 5c). We also capture qualitative trends in function, such as the lower expression of 216UAG-sfGFP from A6_CU-CL_34-1. These results show that our platform can express UAG suppressors identified in metagenomic data and assess their function.

Finally, we aimed to identify the *E. coli* aaRS responsible for aminoacylating these tRNAs. Purified 216UAG-sfGFP from CFPS reactions containing these tRNAs all displayed a mass shift of +27 Da compared to the WT (Figure 5d). This mass shift is consistent with a T216 > Q substitution, suggesting that these tRNAs are nonspecifically recognized by endogenous *E. coli* GlnRS. To confirm that these tRNAs are substrates for GlnRS, we performed an aminoacylation assay that detects an aminoacylated adenosine of interest by LC−MS. In this assay, tRNAs are aminoacylated by an aaRS of interest and digested with RNase A, liberating an aminoacylated adenosine (aa-A, where aa = amino acid).[68,69] Reactions containing GlnRS, glutamine, and a total *E. coli* tRNA mixture resulted in a product with mass (m = 396.1626 Da) identical to gln-A (Figure 5e). Similarly, a product with the same mass and retention time is observed using the six putative UAG suppressors as substrates for GlnRS (Figure 5e). In the absence of either tRNA, GlnRS, or glutamine for all reactions, no product is detected, suggesting the gln-A product. The identity of the gln-A product is also supported by the observation of a second peak existing as a small shoulder to the main peak, which is consistent with equilibration between 2′ and 3′ aminoacylated adenosine products. In total, these data are consistent with nonspecific aminoacylation of UAG suppressors with glutamine by *E. coli* GlnRS.

DISCUSSION

In this work, we developed a cell-free platform to express and evaluate stop codon suppressing tRNAs. This method co-transcribes a tRNA using endogenous *E. coli* machinery alongside an mRNA for a protein of interest to incorporate ncAAs. Our work expands on previous state-of-the-art technologies by showing that a wide variety of orthogonal tRNAs can be expressed by leveraging native tRNA processing sequences in CFPS. UAG- and UAA-suppressing tRNAs, as well as both simultaneously, are compatible with our system. Finally, we use this technology for tRNA characterization and confirm the activity of six putative UAG-suppressors. These UAG-suppressors are nonspecifically aminoacylated with glutamine to support amber suppression.

Our work has several unique features. First, the use of cell-free systems enables rapid protein synthesis (<8 h) in a highly miniaturized form (5 μL) to assess the function of suppressor tRNAs. Even though *in vivo* methods can use life-and-death selections to identify and engineer tRNAs of interest, they are nevertheless bottlenecked by laborious and time-consuming steps afterward, such as colony-picking, outgrowth of a single colony, and 96-well plate-based 216UAG-sfGFP expression during cell growth. Our cell-free workflow bypasses several *in vivo* bottlenecks and enables tRNAs to be assessed more rapidly. We note that cloning a tRNA expression plasmid is required for both approaches. Second, compared to previous cell-free studies, our reactions use naïve cell extracts which enable tRNAs to be screened in a modular format. Finally, our system successfully expresses a broad range of stop-codon suppressing tRNAs, suggesting that it should be a broadly applicable platform to evaluate suppressor tRNAs. In total, this cell-free tRNA expression platform enables simplified expression and characterization of stop codon suppressing tRNAs.

Future developments of our cell-free gene expression platform could seek to improve the activity of UAA suppressor tRNAs and enhance the ability to discover orthogonal tRNAs. For example, for many of the tRNAs tested, UAA suppression resulted in decreased protein synthesis compared to UAG suppression (Figure 3a,c). The precise mechanism for this result is unknown, but it could be that mutating the anticodon from CUA to UUA impacts tRNA expression, maturation, or function. Better understanding of these processes could enable generalizability across a variety of tRNAs and codons. In addition, consistent with the previous literature, we found that GlnRS nonspecifically aminoacylates UAG-suppressing tRNAs.[22,70,71] This points toward a potential challenge in discovering orthogonal tRNAs using our cell-free platform. This challenge could be overcome by several approaches, such as overexpressing native glutamine tRNAs that outcompete UAG suppressors for GlnRS.[71]

Looking forward, we anticipate that our cell-free method to quickly express and characterize tRNAs could be applied to test numerous putative stop-codon suppressing tRNA sequences. As was done in this work, this workflow can be used to test the function of heterologous suppressor tRNAs in *E. coli* cell-free systems. This could be used to test novel tRNAs found in nature, such as those with novel structures.[72] In addition, we are interested in using this workflow to identify orthogonal suppressor tRNAs, which could be accomplished

https://doi.org/10.1021/acschembio.3c00051
ACS Chem. Biol. 2023, 18, 1324−1334

by identifying suppressor tRNAs that do not enable expression of 216UAG-sfGFP. Broadly, this workflow therefore has implications for broadly understanding natural mechanisms for genetic code expansion and for expanding the repertoire of OTSs in synthetic biology.

METHODS

Reagents and Materials. All materials were purchased from Sigma-Aldrich unless otherwise stated. Q5 High-Fidelity DNA Polymerase, DpnI, DNA Loading Dye, T5 Exonuclease, Phusion Polymerase, ET SSB, Taq DNA Ligase, GamS, NEB HiScribe T7 High Yield RNA Synthesis Kit, *E. coli* Inorganic PPIase, and RNase A were purchased from New England Biolabs. Agarose was purchased from Invitrogen. SYBR Safe Dye was purchased from APExBio. DNA was synthesized by either IDT or Twist Biosciences and is specified when described. Nuclease-free water was from Ambion. DH10β chemically competent cells, BL21 (DE3) Star chemically competent cells, Slide-a-Lyzer dialysis cassettes, Pierce protein concentrators, NuPAGE LDS sample buffer, 4−12% bis-tris NuPAGE gels, and MES buffer were purchased from ThermoFisher. AcquaStain protein gel was purchased from Bulldog Bio. Overnight Express TB medium, benzonase, and Amicon Ultra 0.5 mL centrifugal filters were purchased from Millipore. Ammonium glutamate was purchased from MP Bio. Total *E. coli* tRNA and phosphoenolpyruvate were purchased from Roche. Bpy and AzK were purchased from Toronto Research Chemicals. ^{14}C leucine, Filtermat A, and Meltilex A were purchased from Perkin Elmer. Streptactcin XT spin columns were purchased from IBA Life Sciences.

DNA Amplification. All PCRs were conducted using Q5 High-Fidelity DNA Polymerase following the manufacturer's protocols. Primers and gBlocks were synthesized by IDT. The primer sets for each template are listed in Table S1. Thermocycling conditions were performed as described in Table S2 in a Bio-Rad C1000 Touch Thermocycler.

Products from all PCRs were analyzed by agarose gel electrophoresis. Agarose gels were prepared by dissolving agarose in TAE buffer at 1% w/v (for tRNA plasmid backbone amplification and PJL1 backbone amplification) or at 2% w/v (for transzyme amplification) and stained with SYBR Safe dye. The PCR product (2.5 μL) was mixed with 2.5 μL of water and 1 μL of 6X loading dye and loaded into the appropriate agarose gel. Agarose gels (1% w/v) were run at 120 V for 30 min, and 2% w/v agarose gels were run at 120 V for 1 h. Gels were imaged using a Bio-Rad Gel Doc XR+ to confirm the amplicon size.

DNA Assembly. tRNA expression plasmids were assembled using Gibson Assembly. An example sequence of the plasmid containing the *M. jannaschii* $tRNA^{Tyr}_{CUA}$ is provided in Figure S2. The tRNA expression plasmid backbone was amplified as previously described under DNA amplification. PCR reactions were column-purified using Zymo DNA clean and concentrate and resuspended in 10 μL of nuclease-free water. DNA was digested by adding 5 μL of 10X CutSmart buffer, 34 μL of nuclease-free water, and 1 μL of DpnI, then incubated at 37 °C for 1 h followed by 80 °C for 20 min, and then column-purified again. gBlocks containing the tRNA expression cassette, the tRNA, and appropriate overlaps for Gibson Assembly were ordered from Twist Biosciences and are listed in Table S3. The Gibson assembly reaction was prepared by mixing the tRNA plasmid backbone and gBlock in a 1:3 molar ratio, respectively, along with a homemade 3X Gibson Assembly Master Mix (75 mM Tris−HCl pH 7.5, 7.5 mM $MgCl_2$, 0.15 mM dNTPs, 7.5 mM DTT, 0.75 mM NAD, 0.004 U/μL T5 Exonuclease, 0.025 U/μL Phusion polymerase, 4 U/μL Taq DNA ligase, and 3.125 μg/mL ET SSB) and an appropriate volume of water. This mixture was incubated at 50 °C for 1 h. The Gibson assembly reaction (3 μL) was transformed into chemically competent DH10β cells following manufacturer's instructions. Cells were streaked onto LB agar plates containing 50 μg/mL kanamycin and incubated overnight at 37 °C. Single colonies were inoculated into 5 mL of LB-Miller media with 50 μg/mL kanamycin and plasmid DNA was isolated using ZymoPURE Miniprep kits. Accurate assembly of the plasmid was confirmed by Sanger Sequencing at GeneWiz using primers PJL1-Forward (ctgagatacctacagcgtgagc) and PJL1-Reverse (cgtcactcatggtgatttctcacttg).

The 216UAA-sfGFP and 216UAG-212UAA sfGFP were similarly assembled using Gibson Assembly. The PJL1 backbone was amplified using the primer and thermocycling conditions described above. The sfGFP variants containing premature stop codons were synthesized by IDT as gBlocks, and their sequences are listed in Table S3. The insert and backbone were assembled, transformed, and inserts were sequence-verified as described above. Sanger sequencing was done by GeneWiz using their T7-forward and T7-reverse primers.

DNA Purification. Plasmids for all CFPS reactions were purified by ZymoPURE Midiprep kits. Cultures (50 mL) were prepared using LB-Miller media containing kanamycin at 50 μg/mL and were inoculated from single colonies on a plate or from a glycerol stock. DNA was purified following the manufacturer's instructions and was verified by Sanger sequencing as described above.

For transzyme constructs, PCR products were analyzed by agarose gel electrophoresis and column-purified using Zymo DNA clean and concentrate to ∼300 ng/μL.

Cell Extract Preparation. 759.T7 is a genomically engineered *E. coli* strain used in all cell-free experiments in this work. This strain has several features, including (i) all TAG codons that are recoded to TAA, (ii) release factor 1 that was knocked out, (iii) negative effectors (e.g., nucleases) of CFPS that were knocked out, and (iv) T7 RNA polymerase that was integrated onto its genome.[36,37]

A 150 mL overnight culture was inoculated from a glycerol stock and incubated at 34 °C overnight with 250 RPM shaking. The next day, the OD_{600} of a 10X dilution of the overnight culture was measured using a NanoDrop 2000C in a 1 mL cuvette. This was used to inoculate 10 L of 2xYPTG (16 g/L tryptone, 10 g/L yeast extract, 5 g/L NaCl, 7 g/L KH_2PO_4, and 3 g/L K_2HPO_4) at OD_{600} = 0.075 in a 10 L Sartorius Biostat Cplus fermenter at 34 °C. At OD_{600} = 0.5, 10 mL of 1 M IPTG (final concentration = 1 mM) was added to the culture to induce expression of T7 RNA polymerase. Cells were grown until OD_{600} = 3.0. Cells were then harvested by centrifugation (Beckman-Counter Avanti J-26) at 5000 × *g* for 15 min at 4 °C, washed by resuspending with S-30 buffer (10 mM tris-acetate pH 8.2, 14 mM mg of acetate, 60 mM K acetate, 2 mM DTT) and centrifugation at 10,000 × *g* for 2 min for a total of three washes. Cells were pelleted by a final centrifugation at 10,000 × *g* for 5 min at 4 °C. Cells were then flash-frozen at −80 °C until lysis.

Cells were thawed on ice and resuspended in 0.8 mL of S-30 buffer/g wet cell mass by vortexing. Cells were lysed by sonication using a Q125 sonicator (QSonica) at 50% amplitude using 3 × 45 s on and 59 s off cycles to a total of ∼950 J. The lysate was centrifuged at 12,000 × *g* for 10 min at 4 °C to remove insoluble debris. The supernatant was collected and incubated at 37 °C with 250 RPM shaking in a run-off reaction. The lysate was recentrifuged at 12,000 × *g* for 10 min at 4 °C to remove insoluble components that appeared after run-off. Finally, the clarified lysate was dialyzed against 200 volumes of S-30 buffer in a 10 kDa MWCO slide-a-lyzer dialysis cassette. The lysate was then aliquoted into single-use aliquots, flash-frozen in liquid nitrogen, and stored at −80 °C.

aaRS Purification. pET.BCS-BpyRS was cloned as previously described using Gibson Assembly.[73] Expression plasmids for the Chimeric PylRS, the *M. alvus* PylRS, and the *Lum1* PylRS were synthesized in the pET.BCS backbone by Twist Biosciences. pET21a-GlnRS-His was from Addgene (Addgene plasmid # 124109; http://n2t.net/addgene:124109; RRID: Addgene_124109). All aaRSs contained a C-terminal His-tag.

Plasmids were transformed into chemicomp BL21 (DE3) star following the manufacturer's instructions except for GlnRS, which was transformed into BL21 (DE3). Cells were plated onto LB-agar plates containing 100 μg/mL carbenicillin and incubated overnight at 37 °C. A single colony was picked into 5 mL of LB-Carb and grown overnight at 37 °C with 250 RPM shaking. Expression culture (0.25 mL) was inoculated into 250 mL of overnight express TB medium containing carbenicillin and incubated for ∼16 h at 37 °C with 250 RPM shaking. The next day, expression cultures were pelleted by

https://doi.org/10.1021/acschembio.3c00051
ACS Chem. Biol. 2023, 18, 1324−1334

centrifugation at 5000 × *g* for 10 min at 4 °C, washed with Buffer 1 (300 mM NaCl, 50 mM sodium phosphate monobasic pH 8), supplemented with 10 mM imidazole pH 8, pelleted again, and then stored at −80 °C.

Cells were thawed on ice and resuspended in 3 mL of Buffer 1 supplemented with 10 mM imidazole pH 8 and benzonase/g wet cell mass. The cell solution was passed through a syringe needle and lysed by homogenization (Avestin B3) at ∼20,000 PSI. Insoluble components were then pelleted by centrifugation at 20,000 × *g* for 15 min at 4 °C. The supernatant was removed and incubated with 5 mL of pre-equilibrated Ni-NTA resin (Qiagen) for one hour at 4 °C with gentle shaking. The resulting suspension was centrifuged to remove the supernatant at 3800 × *g* for 5 min at 4 °C. The resin was washed five times with 20 mL of Buffer 1 + 20 mM imidazole pH 8 in a 50 mL falcon tube. Finally, the resin was packed into a column, and proteins were eluted from the column using 20 mL of Buffer 1 + 0.5 M imidazole pH 8. Elution fractions containing protein, as measured by A280 on Nanodrop 2000c, were combined and dialyzed overnight into 2 L of Buffer 1 + 40% v/v glycerol with gentle stirring at 4 °C using a slide-a-lyzer dialysis cassette (3.5 kDa MWCO). The dialysis buffer was changed after overnight dialysis and dialyzed for an additional 4 h at 4 °C. Samples were then removed from the dialysis cassette, concentrated using a pierce protein concentrator (3 K MWCO), measured by Nanodrop using extinction coefficients and molecular weights calculated by ExPasy ProtParam, flash-frozen in single use aliquots, and stored at −80 °C.

Protein expression and purity were analyzed by sodium dodecyl sulfate-polyacrylamide gel electrophoresis (SDS-PAGE). Protein (1 μL) was mixed with 3.75 μL of NuPAGE 4X LDS sample buffer, 1.5 μL of 1 M DTT, and water to 15 μL. This sample was denatured at 95 °C for 10 min. Samples were loaded onto a 4−12% bis-tris NuPAGE gel and run in 1X MES buffer for 45 min at 180 V. Gels were stained with gentle shaking using the AcquaStain protein gel for 15 min, destained in water for 1 h, and then imaged.

Cell-Free Protein Synthesis. CFPS reactions are based on a modified PANOx-SP system. Generally, 5 μL of CFPS reactions was set up in 0.2 mL PCR tubes in conditions of 4−12 mM magnesium glutamate, 10 mM ammonium glutamate (MP Bio), 130 mM potassium glutamate, 1.2 mM ATP, 0.85 mM of GTP, CTP, and UTP each, 0.03 mg/mL folinic acid, 0.17 mg/mL tRNA (Roche), 0.4 mM NAD, 0.27 mM CoA, 4 mM oxalic acid, 1 mM putrescine, 1.5 mM spermidine, 57 mM HEPES pH 7.2, 33 mM phosphoenolpyruvate (Roche), and 30% v/v 759.T7 cell extract. The optimal magnesium glutamate concentration was determined for each batch of cell extract. PJL1-sfGFP and tRNA expression plasmids were added at concentrations between 5 and 40 ng/μL as stated in the text. Bpy and AzK (Toronto Research Chemicals) were added at final concentrations of 1 mM, along with 1 mg/mL of the appropriate aaRS (Table 1). For reactions using linear templates, transzyme constructs were added at a final concentration of 30 ng/μL, the WT sfGFP linear template was added in an equal volume as the PJL1-sfGFP plasmid template, and GamS was added at 1 μM. Purified tRNAs were added at a final concentration of 5 μM. Reactions were incubated either at 30 °C or 37 °C as stated in text. Unless otherwise stated, 37 °C was used for suppression of UAG, and 30 °C was used for suppression of UAA and for suppression of both UAG and UAA.

CFPS Quantification of sfGFP. sfGFP concentration in CFPS was quantified by using a standard curve relating sfGFP fluorescence to protein concentration as measured by ^{14}C scintillation counting. WT sfGFP with ^{14}C leucine was synthesized by adding ^{14}C leucine at a final concentration of 10 μM in 15 μL CFPS reactions. CFPS reactions were spun down at 21,000 × *g* for 15 min at 4 °C, and 5 μL of supernatant was removed to isolate soluble proteins. An equal volume of 0.5 M KOH was added to the soluble proteins and incubated at 37 °C for 20 min. Each sample (4 μL) was then spotted onto two Filtermat A fiberglass paper sheets and allowed to dry under a heat lamp. One of the filtermats was washed three times with 5% w/v TCA for 15 min at 4 °C and then washed with 100% ethanol at room temperature for 15 min. The filtermat was again allowed to dry under a heat lamp. Meltilex A was then applied to both filtermats. After cooling and solidifying, scintillation counts were measured using the MicroBeta^2 (Perkin Elmer) and soluble yields were calculated as previously described.[74]

Dilutions of the sfGFP were made in 1X PBS and measured on a plate reader (BioTek Synergy 2). A standard curve was built using linear regression to fit fluorescence measurements to yields as calculated by ^{14}C scintillation counting.

Preparation of Proteins for Intact Protein ESI-MS. Proteins were synthesized using CFPS as described in sections above, except that reactions were scaled up to 75 or 150 μL CFPS reactions in a 50 mL falcon tube. Proteins were purified from CFPS reactions using Strep-Tactin XT spin columns according to the manufacturer's instructions. Proteins were then buffer-exchanged into 0.1 M ammonium acetate using Amicon ultra 0.5 mL centrifugal filters (10 kDa MWCO).

Proteins were analyzed with ESI-MS as described in previous publications with slight modifications.[30] Eight microliters of 2 μM purified, buffer-exchanged protein (16 pmol) were injected into a Bruker Elite UPLC coupled to a Bruker Impact II UHR TOF mass spectrometer. Proteins were deconvoluted using a *m/z* range of 20,000−30,000 Da. Data were plotted using a custom Python script provided in the github link below.

***In Vitro* Transcription of tRNAs.** Templates for *in vitro* transcription (IVT) of tRNAs were amplified with a 400 μL PCR reaction as described in previous sections. The template was designed in a transzyme format to enable efficient transcription of the tRNAs.[51] PCR products were analyzed by agarose gel electrophoresis to confirm amplification. PCR reactions were column-purified using a Zymo DNA Clean and Concentrate kit, with a yield of ∼3 μg. All products were added to a 200 μL *in vitro* transcription reaction using the NEB HiScribe T7 High Yield RNA Synthesis Kit at 0.75X concentration as recommended due to the size of the template DNA. Reactions were incubated at 37 °C overnight. The next day, reactions were diluted with 1 mL of NF-water and incubated at 60 °C for one hour for ribozyme cleavage.

IVT reactions were purified by ethanol precipitation and gel purification. 0.1X volumes of 3 M NaCl and 2.5X volumes of 100%, ice-cold ethanol were mixed into the reactions. Nucleic acids were pelleted by centrifugation at 21 k × *g* for 5 min at 4 °C. Reactions were washed twice with 500 μL of ice-cold 70% ethanol, dried, and then resuspended in 100 μL of nuclease-free water. Resuspended nucleic acids were stored at −80 °C or used immediately. Gel casters were plugged with a solution of 3% w/v agarose solution. While the plug was solidifying, a 20 mL solution of 7.5% acrylamide, 7 M urea, and 1X TBE buffer was prepared. When the plug solidified, this solution was mixed with 200 μL of 10% w/v APS and 20 μL of TEMED and immediately poured into gel casters using 1 mm spacers and allowed to polymerize for ∼45 min. After solidifying, the gel was pre-run in 1X TBE buffer at 250 V for 15 min. The resuspended nucleic acids were then mixed with 100 μL of gel-loading buffer (8 M urea, 2 mM Tris pH 7.5, 2 mM EDTA, 0.004% bromophenol blue), incubated at 70 °C for 10 min, and then cooled on ice for 5 min. Samples were then loaded onto the gel and run at 250 V for 2 h. Bands corresponding to the expected tRNA size were identified by UV shadowing and excised from the gel. The excised gel was crushed and incubated with 1.5 mL of NF-water in a 15 mL falcon tube overnight at 4 °C with end-over-end shaking. Tubes were centrifuged at 4 k × *g* for 5 min to pellet gel, and the supernatant was collected. RNA from the supernatant was purified by ethanol precipitation, resuspended in NF-water, and quantified by Nanodrop. tRNAs were stored at −80 °C.

Aminoacylation of tRNAs by GlnRS. Aminoacylation reactions were set up by mixing 2 μL of 5X assay buffer (0.5 M HEPES-K pH 7.5, 20 mM DTT, 50 mM $MgCl_2$, and 50 mM ATP), 0.4 μL of 100 U/mL PPIase, 1 μL of 25 mM Gln, 0.63 μL of 40 μM GlnRS, 3 μL of 15 μM purified tRNA, and water to 10 μL final volume. Reactions were incubated at 37 °C for 2 h. Reactions were quenched with 1.1 volumes of RNase A solution (200 mM sodium acetate pH 5.2, 1.5 U/μL RNase A), mixed well, and incubated at room temperature for

https://doi.org/10.1021/acschembio.3c00051
ACS Chem. Biol. 2023, 18, 1324−1334

five minutes. Reactions were treated with 0.1 volumes of 50% w/v trichloroacetic acid and then frozen at −80 °C for at least 30 min.

Samples were spun down at 21,000 × *g* for 10 min at 4 °C, and the supernatant was transferred to autosampler vials and analyzed by LC−MS. Samples were injected on a 1290 Infinity II UHPLC System (Agilent Technologies Inc., Santa Clara, California, USA) onto a Poroshell 120 EC-C18 column (1.9 μm, 50 × 2.1 mm) (Agilent Technologies Inc., Santa Clara, California, USA) for reverse-phase separation which was maintained at 30 °C with a constant flow rate at 0.500 mL/min, using a gradient of mobile phase A (water, 0.1% formic acid (v/v)) and mobile phase B (acetonitrile, 0.1% formic acid (v/v)). The gradient program was as follows: 0−1 min, 2%B; 1−5 min, 2−40%B; 5−6 min, 40−99%B; 6−8 mins, 99%B; 8−8.10 min, 99−2%B; 8.10−14 min, 2%B. "MS-Only," positive ion mode acquisition was utilized on an Agilent 6545 quadrupole time-of-flight mass spectrometer equipped with a JetStream ionization source (Agilent Technologies Inc., Santa Clara, California, USA). The source conditions were as follows: gas temperature, 300 °C; drying gas flow, 12 L/ min; nebulizer, 45 psi; sheath gas temperature, 350 °C; sheath gas flow, 12 L/ min; VCap, 3500 V; fragmentor, 110 V; skimmer, 65 V; and oct 1 RF, 750 V. The acquisition rate in MS-Only mode was 3 spectra/second, utilizing *m/z* 121.050873 and *m/z* 922.009798 as reference masses. Samples were scanned for masses corresponding to the formula $C_{15}H_{21}N_7O_6$. Data were plotted using a custom Python script provided in the github link below.

■ ASSOCIATED CONTENT

Supporting Information

The Supporting Information is available free of charge at https://pubs.acs.org/doi/10.1021/acschembio.3c00051.

Additional experimental results and DNA sequences (PDF)

Formatted raw data and details of raw data (XLSX)

■ AUTHOR INFORMATION

Corresponding Author

Michael C. Jewett − *Department of Chemical and Biological Engineering, Chemistry of Life Processes Institute, and Center for Synthetic Biology, Northwestern University, Evanston, Illinois 60208, United States; Robert H. Lurie Comprehensive Cancer Center and Simpson Querrey Institute, Northwestern University, Chicago, Illinois 60611, United States;* orcid.org/0000-0003-2948-6211; Email: m-jewett@northwestern.edu

Authors

Kosuke Seki − *Department of Chemical and Biological Engineering, Chemistry of Life Processes Institute, and Center for Synthetic Biology, Northwestern University, Evanston, Illinois 60208, United States;* orcid.org/0000-0002-0413-8184

Joey L. Galindo − *Department of Chemical and Biological Engineering, Chemistry of Life Processes Institute, and Center for Synthetic Biology, Northwestern University, Evanston, Illinois 60208, United States*

Ashty S. Karim − *Department of Chemical and Biological Engineering, Chemistry of Life Processes Institute, and Center for Synthetic Biology, Northwestern University, Evanston, Illinois 60208, United States*

Complete contact information is available at: https://pubs.acs.org/10.1021/acschembio.3c00051

Funding

This work was supported by the Army Research Office (W911NF-18-1-0200).

Notes

The authors declare the following competing financial interest(s): M.C.J. has a financial interest in SwiftScale Biologics, Gauntlet Bio, Pearl Bio, Inc., Design Pharmaceutics, and Stemloop Inc. M.C.J.'s interests are reviewed and managed by Northwestern University in accordance with their competing interest policies. All other authors declare no competing interests.

Custom python codes for Figures 2−5 are deposited under https://github.com/kosukeseki/Cell_free_tRNA_Expression

The data underlying this study are available in the published article and its Supporting Information.

■ ACKNOWLEDGMENTS

The authors would like to acknowledge A. Hunt, S. Fleming, C. Kofman, J. Willi, and A. Krüger for helpful scientific discussion, J. Jung for assistance with tRNA purification, J. Hershewe for plasmid design, and B. Owen and F. Tobias for training and assistance with mass spectrometry. This work made use of the IMSERC MS facility at Northwestern University, which has received support from the Soft and Hybrid Nanotechnology Experimental (SHyNE) Resource (NSF ECCS-2025633) and Northwestern University.

■ REFERENCES

(1) Wang, Y.; Xue, P.; Cao, M.; Yu, T.; Lane, S. T.; Zhao, H. Directed Evolution: Methodologies and Applications. *Chem. Rev.* **2021**, *121*, 12384−12444.

(2) Kofman, C.; Lee, J.; Jewett, M. C. Engineering Molecular Translation Systems. *Cell Syst.* **2021**, *12*, 593−607.

(3) de la Torre, D.; Chin, J. W. Reprogramming the Genetic Code. *Nat. Rev. Genet.* **2021**, *22*, 169−184.

(4) Arranz-Gibert, P.; Vanderschuren, K.; Isaacs, F. J. Next-Generation Genetic Code Expansion. *Curr. Opin. Chem. Biol.* **2018**, *46*, 203−211.

(5) Young, D. D.; Schultz, P. G. Playing with the Molecules of Life. *ACS Chem. Biol.* **2018**, *13*, 854−870.

(6) Katoh, T.; Suga, H. In Vitro Genetic Code Reprogramming for the Expansion of Usable Noncanonical Amino Acids. *Annu. Rev. Biochem.* **2022**, *91*, 221−243.

(7) Burke, A. J.; Lovelock, S. L.; Frese, A.; Crawshaw, R.; Ortmayer, M.; Dunstan, M.; Levy, C.; Green, A. P. Design and Evolution of an Enzyme with a Non-Canonical Organocatalytic Mechanism. *Nature* **2019**, *570*, 219−223.

(8) Pott, M.; Tinzl, M.; Hayashi, T.; Ota, Y.; Dunkelmann, D.; Mittl, P. R. E.; Hilvert, D. Noncanonical Heme Ligands Steer Carbene Transfer Reactivity in an Artificial Metalloenzyme. *Angew. Chem. Int. Ed.* **2021**, *133*, 15190−15195.

(9) Hayashi, A.; Haruna, K.-I.; Sato, H.; Ito, K.; Makino, C.; Ito, T.; Sakamoto, K. Incorporation of Halogenated Amino Acids into Antibody Fragments at Multiple Specific Sites Enhances Antigen Binding. *ChemBioChem* **2021**, *22*, 120−123.

(10) Islam, M.; Kehoe, H. P.; Lissoos, J. B.; Huang, M.; Ghadban, C. E.; Berumen Sánchez, G.; Lane, H. Z.; Van Deventer, J. A. Chemical Diversification of Simple Synthetic Antibodies. *ACS Chem. Biol.* **2021**, *16*, 344−359.

(11) Costa, S. A.; Simon, J. R.; Amiram, M.; Tang, L.; Zauscher, S.; Brustad, E. M.; Isaacs, F. J.; Chilkoti, A. Photo-Crosslinkable Unnatural Amino Acids Enable Facile Synthesis of Thermoresponsive Nano- to Microgels of Intrinsically Disordered Polypeptides. *Adv. Mater.* **2018**, *30*, No. 1704878.

(12) Shapiro, D. M.; Mandava, G.; Yalcin, S. E.; Arranz-Gibert, P.; Dahl, P. J.; Shipps, C.; Gu, Y.; Srikanth, V.; Salazar-Morales, A. I.; O'Brien, J. P.; Vanderschuren, K.; Vu, D.; Batista, V. S.; Malvankar, N. S.; Isaacs, F. J. Protein Nanowires with Tunable Functionality and

Programmable Self-Assembly Using Sequence-Controlled Synthesis. *Nat. Commun.* **2022**, *13*, 829.
(13) Hershewe, J. M.; Wiseman, W. D.; Kath, J. E.; Buck, C. C.; Gupta, M. K.; Dennis, P. B.; Naik, R. R.; Jewett, M. C. Characterizing and Controlling Nanoscale Self-Assembly of Suckerin-12. *ACS Synth. Biol.* **2020**, *9*, 3388−3399.
(14) Vanderschuren, K.; Arranz-Gibert, P.; Khang, M.; Hadar, D.; Gaudin, A.; Yang, F.; Folta-Stogniew, E.; Saltzman, W. M.; Amiram, M.; Isaacs, F. J. Tuning Protein Half-Life in Mouse Using Sequence-Defined Biopolymers Functionalized with Lipids. *Proc. Natl. Acad. Sci. U. S. A.* **2022**, *119*, No. e2103099119.
(15) Huang, Y.; Wiedmann, M. M.; Suga, H. RNA Display Methods for the Discovery of Bioactive Macrocycles. *Chem. Rev.* **2019**, *119*, 10360−10391.
(16) Thyer, R.; Ellington, A. D. The Role of tRNA in Establishing New Genetic Codes. *Biochemistry* **2019**, *58*, 1460−1463.
(17) Krahn, N.; Tharp, J. M.; Crnković, A.; Söll, D. Engineering Aminoacyl-tRNA Synthetases for Use in Synthetic Biology. *Enzymes* **2020**, *48*, 351−395.
(18) Willis, J. C. W.; Chin, J. W. Mutually Orthogonal Pyrrolysyl-tRNA Synthetase/tRNA Pairs. *Nat. Chem.* **2018**, *10*, 831−837.
(19) Dunkelmann, D. L.; Willis, J. C. W.; Beattie, A. T.; Chin, J. W. Engineered Triply Orthogonal Pyrrolysyl-tRNA Synthetase/tRNA Pairs Enable the Genetic Encoding of Three Distinct Non-Canonical Amino Acids. *Nat. Chem.* **2020**, *12*, 535−544.
(20) Cervettini, D.; Tang, S.; Fried, S. D.; Willis, J. C. W.; Funke, L. F. H.; Colwell, L. J.; Chin, J. W. Rapid Discovery and Evolution of Orthogonal Aminoacyl-tRNA Synthetase-TRNA Pairs. *Nat. Biotechnol.* **2020**, *38*, 989−999.
(21) Zambaldo, C.; Koh, M.; Nasertorabi, F.; Han, G. W.; Chatterjee, A.; Stevens, R. C.; Schultz, P. G. An Orthogonal Seryl-tRNA Synthetase/tRNA Pair for Noncanonical Amino Acid Mutagenesis in Escherichia Coli. *Bioorg. Med. Chem.* **2020**, *28*, No. 115662.
(22) Italia, J. S.; Addy, P. S.; Wrobel, C. J. J.; Crawford, L. A.; Lajoie, M. J.; Zheng, Y.; Chatterjee, A. An Orthogonalized Platform for Genetic Code Expansion in Both Bacteria and Eukaryotes. *Nat. Chem. Biol.* **2017**, *13*, 446−450.
(23) Dunkelmann, D. L.; Oehm, S. B.; Beattie, A. T.; Chin, J. W. A 68-Codon Genetic Code to Incorporate Four Distinct Non-Canonical Amino Acids Enabled by Automated Orthogonal mRNA Design. *Nat. Chem.* **2021**, *13*, 1110−1117.
(24) Tharp, J. M.; Vargas-Rodriguez, O.; Schepartz, A.; Söll, D. Genetic Encoding of Three Distinct Noncanonical Amino Acids Using Reprogrammed Initiator and Nonsense Codons. *ACS Chem. Biol.* **2021**, *16*, 766−774.
(25) Fischer, J. T.; Söll, D.; Tharp, J. M. Directed Evolution of Methanomethylophilus Alvus Pyrrolysyl-tRNA Synthetase Generates a Hyperactive and Highly Selective Variant. *Front. Mol. Biosci.* **2022**, *9*, No. 850613.
(26) Italia, J. S.; Addy, P. S.; Erickson, S. B.; Peeler, J. C.; Weerapana, E.; Chatterjee, A. Mutually Orthogonal Nonsense-Suppression Systems and Conjugation Chemistries for Precise Protein Labeling at up to Three Distinct Sites. *J. Am. Chem. Soc.* **2019**, *141*, 6204−6212.
(27) Amiram, M.; Haimovich, A. D.; Fan, C.; Wang, Y.-S.; Aerni, H.-R.; Ntai, I.; Moonan, D. W.; Ma, N. J.; Rovner, A. J.; Hong, S. H.; Kelleher, N. L.; Goodman, A. L.; Jewett, M. C.; Söll, D.; Rinehart, J.; Isaacs, F. J. Evolution of Translation Machinery in Recoded Bacteria Enables Multi-Site Incorporation of Nonstandard Amino Acids. *Nat. Biotechnol.* **2015**, *33*, 1272−1279.
(28) Ellefson, J. W.; Meyer, A. J.; Hughes, R. A.; Cannon, J. R.; Brodbelt, J. S.; Ellington, A. D. Directed Evolution of Genetic Parts and Circuits by Compartmentalized Partnered Replication. *Nat. Biotechnol.* **2014**, *32*, 97−101.
(29) Silverman, A. D.; Karim, A. S.; Jewett, M. C. Cell-Free Gene Expression: An Expanded Repertoire of Applications. *Nat. Rev. Genet.* **2020**, *21*, 151−170.
(30) Kightlinger, W.; Duncker, K. E.; Ramesh, A.; Thames, A. H.; Natarajan, A.; Stark, J. C.; Yang, A.; Lin, L.; Mrksich, M.; DeLisa, M. P.; Jewett, M. C. A Cell-Free Biosynthesis Platform for Modular Construction of Protein Glycosylation Pathways. *Nat. Commun.* **2019**, *10*, 5404.
(31) Vögeli, B.; Schulz, L.; Garg, S.; Tarasava, K.; Clomburg, J. M.; Lee, S. H.; Gonnot, A.; Moully, E. H.; Kimmel, B. R.; Tran, L.; Zeleznik, H.; Brown, S. D.; Simpson, S. D.; Mrksich, M.; Karim, A. S.; Gonzalez, R.; Köpke, M.; Jewett, M. C. Cell-Free Prototyping Enables Implementation of Optimized Reverse β-Oxidation Pathways in Heterotrophic and Autotrophic Bacteria. *Nat. Commun.* **2022**, *13*, 3058.
(32) Liew, F. E.; Nogle, R.; Abdalla, T.; Rasor, B. J.; Canter, C.; Jensen, R. O.; Wang, L.; Strutz, J.; Chirania, P.; De Tissera, S.; Mueller, A. P.; Ruan, Z.; Gao, A.; Tran, L.; Engle, N. L.; Bromley, J. C.; Daniell, J.; Conrado, R.; Tschaplinski, T. J.; Giannone, R. J.; Hettich, R. L.; Karim, A. S.; Simpson, S. D.; Brown, S. D.; Leang, C.; Jewett, M. C.; Köpke, M. Carbon-Negative Production of Acetone and Isopropanol by Gas Fermentation at Industrial Pilot Scale. *Nat. Biotechnol.* **2022**, *40*, 335−344.
(33) Karim, A. S.; Dudley, Q. M.; Juminaga, A.; Yuan, Y.; Crowe, S. A.; Heggestad, J. T.; Garg, S.; Abdalla, T.; Grubbe, W. S.; Rasor, B. J.; Coar, D. N.; Torculas, M.; Krein, M.; Liew, F. E.; Quattlebaum, A.; Jensen, R. O.; Stuart, J. A.; Simpson, S. D.; Köpke, M.; Jewett, M. C. In Vitro Prototyping and Rapid Optimization of Biosynthetic Enzymes for Cell Design. *Nat. Chem. Biol.* **2020**, *16*, 912−919.
(34) Hunt, A. C.; Case, J. B.; Park, Y.-J.; Cao, L.; Wu, K.; Walls, A. C.; Liu, Z.; Bowen, J. E.; Yeh, H.-W.; Saini, S.; Helms, L.; Zhao, Y. T.; Hsiang, T.-Y.; Starr, T. N.; Goreshnik, I.; Kozodoy, L.; Carter, L.; Ravichandran, R.; Green, L. B.; Matochko, W. L.; Thomson, C. A.; Vögeli, B.; Krüger, A.; VanBlargan, L. A.; Chen, R. E.; Ying, B.; Bailey, A. L.; Kafai, N. M.; Boyken, S. E.; Ljubetič, A.; Edman, N.; Ueda, G.; Chow, C. M.; Johnson, M.; Addetia, A.; Navarro, M. J.; Panpradist, N.; Gale, M., Jr.; Freedman, B. S.; Bloom, J. D.; Ruohola-Baker, H.; Whelan, S. P. J.; Stewart, L.; Diamond, M. S.; Veesler, D.; Jewett, M. C.; Baker, D. Multivalent Designed Proteins Neutralize SARS-CoV-2 Variants of Concern and Confer Protection against Infection in Mice. *Sci. Transl. Med.* **2022**, *14*, No. eabn1252.
(35) Hunt, A. C.; Vögeli, B.; Kightlinger, W. K.; Yoesep, D. J.; Krüger, A.; Jewett, M. C. A High-Throughput, Automated, Cell-Free Expression and Screening Platform for Antibody Discovery. *bioRxiv* **2021**, DOI: 10.1101/2021.11.04.467378.
(36) Martin, R. W.; Des Soye, B. J.; Kwon, Y.-C.; Kay, J.; Davis, R. G.; Thomas, P. M.; Majewska, N. I.; Chen, C. X.; Marcum, R. D.; Weiss, M. G.; Stoddart, A. E.; Amiram, M.; Ranji Charna, A. K.; Patel, J. R.; Isaacs, F. J.; Kelleher, N. L.; Hong, S. H.; Jewett, M. C. Cell-Free Protein Synthesis from Genomically Recoded Bacteria Enables Multisite Incorporation of Noncanonical Amino Acids. *Nat. Commun.* **2018**, *9*, 1203.
(37) Des Soye, B. J.; Gerbasi, V. R.; Thomas, P. M.; Kelleher, N. L.; Jewett, M. C. A Highly Productive, One-Pot Cell-Free Protein Synthesis Platform Based on Genomically Recoded Escherichia Coli. *Cell Chem. Biol.* **2019**, *26*, 1743−1754.e9.
(38) Quast, R. B.; Mrusek, D.; Hoffmeister, C.; Sonnabend, A.; Kubick, S. Cotranslational Incorporation of Non-Standard Amino Acids Using Cell-Free Protein Synthesis. *FEBS Lett.* **2015**, *589*, 1703−1712.
(39) Bundy, B. C.; Swartz, J. R. Site-Specific Incorporation of p-Propargyloxyphenylalanine in a Cell-Free Environment for Direct Protein-Protein Click Conjugation. *Bioconjugate Chem.* **2010**, *21*, 255−263.
(40) Worst, E. G.; Exner, M. P.; De Simone, A.; Schenkelberger, M.; Noireaux, V.; Budisa, N.; Ott, A. Cell-Free Expression with the Toxic Amino Acid Canavanine. *Bioorg. Med. Chem. Lett.* **2015**, *25*, 3658−3660.
(41) Lee, J.; Coronado, J. N.; Cho, N.; Lim, J.; Hosford, B. M.; Seo, S.; Kim, D. S.; Kofman, C.; Moore, J. S.; Ellington, A. D.; Anslyn, E. V.; Jewett, M. C. Ribosome-Mediated Biosynthesis of Pyridazinone Oligomers in Vitro. *Nat. Commun.* **2022**, *13*, 6322.
(42) Lee, J.; Schwarz, K. J.; Kim, D. S.; Moore, J. S.; Jewett, M. C. Ribosome-Mediated Polymerization of Long Chain Carbon and

Cyclic Amino Acids into Peptides in Vitro. *Nat. Commun.* **2020**, *11*, 4304.
(43) Lee, J.; Torres, R.; Kim, D. S.; Byrom, M.; Ellington, A. D.; Jewett, M. C. Ribosomal Incorporation of Cyclic β-Amino Acids into Peptides Using in Vitro Translation. *Chem. Commun.* **2020**, *56*, 5597−5600.
(44) Ozer, E.; Chemla, Y.; Schlesinger, O.; Aviram, H. Y.; Riven, I.; Haran, G.; Alfonta, L. In Vitro Suppression of Two Different Stop Codons. *Biotechnol. Bioeng.* **2017**, *114*, 1065−1073.
(45) Cui, Z.; Mureev, S.; Polinkovsky, M. E.; Tnimov, Z.; Guo, Z.; Durek, T.; Jones, A.; Alexandrov, K. Combining Sense and Nonsense Codon Reassignment for Site-Selective Protein Modification with Unnatural Amino Acids. *ACS Synth. Biol.* **2017**, *6*, 535−544.
(46) Cui, Z.; Wu, Y.; Mureev, S.; Alexandrov, K. Oligonucleotide-Mediated tRNA Sequestration Enables One-Pot Sense Codon Reassignment in Vitro. *Nucleic Acids Res.* **2018**, *46*, 6387−6400.
(47) Lee, K. B.; Kim, H.-C.; Kim, D.-M.; Kang, T. J.; Suga, H. Comparative Evaluation of Two Cell-Free Protein Synthesis Systems Derived from Escherichia Coli for Genetic Code Reprogramming. *J. Biotechnol.* **2012**, *164*, 330−335.
(48) Lee, K. B.; Hou, C. Y.; Kim, C.-E.; Kim, D.-M.; Suga, H.; Kang, T. J. Genetic Code Expansion by Degeneracy Reprogramming of Arginyl Codons. *ChemBioChem* **2016**, *17*, 1198−1201.
(49) Zimmerman, E. S.; Heibeck, T. H.; Gill, A.; Li, X.; Murray, C. J.; Madlansacay, M. R.; Tran, C.; Uter, N. T.; Yin, G.; Rivers, P. J.; Yam, A. Y.; Wang, W. D.; Steiner, A. R.; Bajad, S. U.; Penta, K.; Yang, W.; Hallam, T. J.; Thanos, C. D.; Sato, A. K. Production of Site-Specific Antibody-Drug Conjugates Using Optimized Non-Natural Amino Acids in a Cell-Free Expression System. *Bioconjugate Chem.* **2014**, *25*, 351−361.
(50) Albayrak, C.; Swartz, J. R. Cell-Free Co-Production of an Orthogonal Transfer RNA Activates Efficient Site-Specific Non-Natural Amino Acid Incorporation. *Nucleic Acids Res.* **2013**, *41*, 5949−5963.
(51) Fechter, P.; Rudinger, J.; Giegé, R.; Théobald-Dietrich, A. Ribozyme Processed tRNA Transcripts with Unfriendly Internal Promoter for T7 RNA Polymerase: Production and Activity. *FEBS Lett.* **1998**, *436*, 99−103.
(52) Wan, W.; Huang, Y.; Wang, Z.; Russell, W. K.; Pai, P.-J.; Russell, D. H.; Liu, W. R. A Facile System for Genetic Incorporation of Two Different Noncanonical Amino Acids into One Protein in Escherichia Coli. *Angew. Chem. Int. Ed.* **2010**, *49*, 3211−3214.
(53) Sun, Z. Z.; Yeung, E.; Hayes, C. A.; Noireaux, V.; Murray, R. M. Linear DNA for Rapid Prototyping of Synthetic Biological Circuits in an Escherichia Coli Based TX-TL Cell-Free System. *ACS Synth. Biol.* **2014**, *3*, 387−397.
(54) Jewett, M. C.; Calhoun, K. A.; Voloshin, A.; Wuu, J. J.; Swartz, J. R. An Integrated Cell-Free Metabolic Platform for Protein Production and Synthetic Biology. *Mol. Syst. Biol.* **2008**, *4*, 220.
(55) Xie, J.; Liu, W.; Schultz, P. G. A Genetically Encoded Bidentate, Metal-Binding Amino Acid. *Angew. Chem. Int. Ed.* **2007**, *46*, 9239−9242.
(56) Bryson, D. I.; Fan, C.; Guo, L.-T.; Miller, C.; Söll, D.; Liu, D. R. Continuous Directed Evolution of Aminoacyl-tRNA Synthetases. *Nat. Chem. Biol.* **2017**, *13*, 1253−1260.
(57) Chatterjee, A.; Sun, S. B.; Furman, J. L.; Xiao, H.; Schultz, P. G. A Versatile Platform for Single- and Multiple-Unnatural Amino Acid Mutagenesis in Escherichia Coli. *Biochemistry* **2013**, *52*, 1828−1837.
(58) Ryu, Y.; Schultz, P. G. Efficient Incorporation of Unnatural Amino Acids into Proteins in Escherichia Coli. *Nat. Methods* **2006**, *3*, 263−265.
(59) Jewett, M. C.; Fritz, B. R.; Timmerman, L. E.; Church, G. M. In Vitro Integration of Ribosomal RNA Synthesis, Ribosome Assembly, and Translation. *Mol. Syst. Biol.* **2013**, *9*, 678.
(60) Aerni, H. R.; Shifman, M. A.; Rogulina, S.; O'Donoghue, P.; Rinehart, J. Revealing the Amino Acid Composition of Proteins within an Expanded Genetic Code. *Nucleic Acids Res.* **2015**, *43*, No. e8.
(61) Muskhelishvili, G.; Buckle, M.; Heumann, H.; Kahmann, R.; Travers, A. A. FIS Activates Sequential Steps during Transcription Initiation at a Stable RNA Promoter. *EMBO J.* **1997**, *16*, 3655−3665.
(62) O'Donoghue, P.; Prat, L.; Heinemann, I. U.; Ling, J.; Odoi, K.; Liu, W. R.; Söll, D. Near-Cognate Suppression of Amber, Opal and Quadruplet Codons Competes with Aminoacyl-tRNAPyl for Genetic Code Expansion. *FEBS Lett.* **2012**, *586*, 3931−3937.
(63) Venkat, S.; Sturges, J.; Stahman, A.; Gregory, C.; Gan, Q.; Fan, C. Genetically Incorporating Two Distinct Post-Translational Modifications into One Protein Simultaneously. *ACS Synth. Biol.* **2018**, *7*, 689−695.
(64) Wan, W.; Tharp, J. M.; Liu, W. R. Pyrrolysyl-TRNA Synthetase: An Ordinary Enzyme but an Outstanding Genetic Code Expansion Tool. *Biochim. Biophys. Acta* **2014**, *1844*, 1059−1070.
(65) Nozawa, K.; O'Donoghue, P.; Gundllapalli, S.; Araiso, Y.; Ishitani, R.; Umehara, T.; Söll, D.; Nureki, O. Pyrrolysyl-tRNA Synthetase-TRNA(Pyl) Structure Reveals the Molecular Basis of Orthogonality. *Nature* **2009**, *457*, 1163−1167.
(66) Bednar, R. M.; Jana, S.; Kuppa, S.; Franklin, R.; Beckman, J.; Antony, E.; Cooley, R. B.; Mehl, R. A. Genetic Incorporation of Two Mutually Orthogonal Bioorthogonal Amino Acids That Enable Efficient Protein Dual-Labeling in Cells. *ACS Chem. Biol.* **2021**, *16*, 2612−2622.
(67) Al-Shayeb, B.; Sachdeva, R.; Chen, L.-X.; Ward, F.; Munk, P.; Devoto, A.; Castelle, C. J.; Olm, M. R.; Bouma-Gregson, K.; Amano, Y.; He, C.; Méheust, R.; Brooks, B.; Thomas, A.; Lavy, A.; Matheus-Carnevali, P.; Sun, C.; Goltsman, D. S. A.; Borton, M. A.; Sharrar, A.; Jaffe, A. L.; Nelson, T. C.; Kantor, R.; Keren, R.; Lane, K. R.; Farag, I. F.; Lei, S.; Finstad, K.; Amundson, R.; Anantharaman, K.; Zhou, J.; Probst, A. J.; Power, M. E.; Tringe, S. G.; Li, W.-J.; Wrighton, K.; Harrison, S.; Morowitz, M.; Relman, D. A.; Doudna, J. A.; Lehours, A.-C.; Warren, L.; Cate, J. H. D.; Santini, J. M.; Banfield, J. F. Clades of Huge Phages from across Earth's Ecosystems. *Nature* **2020**, *578*, 425−431.
(68) McMurry, J. L.; Chang, M. C. Y. Fluorothreonyl-tRNA Deacylase Prevents Mistranslation in the Organofluorine Producer Streptomyces Cattleya. *Proc. Natl. Acad. Sci. U. S. A.* **2017**, *114*, 11920−11925.
(69) Ad, O.; Hoffman, K. S.; Cairns, A. G.; Featherston, A. L.; Miller, S. J.; Söll, D.; Schepartz, A. Translation of Diverse Aramid- and 1,3-Dicarbonyl-Peptides by Wild Type Ribosomes in Vitro. *ACS Cent. Sci.* **2019**, *5*, 1289−1294.
(70) Swanson, R.; Hoben, P.; Sumner-Smith, M.; Uemura, H.; Watson, L.; Söll, D. Accuracy of in Vivo Aminoacylation Requires Proper Balance of tRNA and Aminoacyl-tRNA Synthetase. *Science* **1988**, *242*, 1548−1551.
(71) Italia, J. S.; Latour, C.; Wrobel, C. J. J.; Chatterjee, A. Resurrecting the Bacterial Tyrosyl-tRNA Synthetase/tRNA Pair for Expanding the Genetic Code of Both E. coli and Eukaryotes. *Cell Chem. Biol.* **2018**, *25*, 1304−1312.e5.
(72) Mukai, T.; Vargas-Rodriguez, O.; Englert, M.; Tripp, H. J.; Ivanova, N. N.; Rubin, E. M.; Kyrpides, N. C.; Söll, D. Transfer RNAs with Novel Cloverleaf Structures. *Nucleic Acids Res.* **2017**, *45*, 2776−2785.
(73) Zubi, Y. S.; Seki, K.; Li, Y.; Hunt, A. C.; Liu, B.; Roux, B.; Jewett, M. C.; Lewis, J. C. Metal-Responsive Regulation of Enzyme Catalysis Using Genetically Encoded Chemical Switches. *Nat. Commun.* **2022**, *13*, 1864.
(74) Swartz, J. R.; Jewett, M. C.; Woodrow, K. A. Cell-Free Protein Synthesis With Prokaryotic Combined Transcription-Translation. In *Recombinant Gene Expression: Reviews and Protocols*; Balbás, P., Lorence, A., Eds.; Humana Press: Totowa, NJ, 2004; pp. 169−182.

https://doi.org/10.1021/acschembio.3c00051
ACS Chem. Biol. 2023, 18, 1324−1334